Biochemical and Biophysical Research Communications **288,** 263–268 (2001)
doi:10.1006/bbrc.2001.5752, available online at http://www.idealibrary.com on IDEAL®

Mutational Effects on Thermostable Superoxide Dismutase from *Aquifex pyrophilus:* Understanding the Molecular Basis of Protein Thermostability

Jae-Hwan Lim,* Kwang Yeon Hwang,† Juhyun Choi,*,‡ Duck Yeon Lee,* Byung-Yoon Ahn,‡ Yunje Cho,§ Key-Sun Kim,* and Ye Sun Han*,[1]

**Structural Biology Research Center, Korea Institute of Science and Technology, Seoul, Korea; †Crystal Genomics Incorporated, Taejon, Korea; ‡Department of Genetic Engineering, Korea University, Seoul, Korea; and §Department of Life Science, Pohang University of Science and Technology, Pohang, Korea*

Received September 18, 2001

We designed two mutants of superoxide dismutase (SOD), one is thermostable and the other is thermolabile, which provide valuable insight to identify amino acid residues essential for the thermostability of the SOD from *Aquifex pyrophilus* (*Ap*SOD). The mutant K12A, in which Lys12 was replaced by Ala, had increased thermostability compared to that of the wild type. The $T_{1/2}$ value of K12A was 210 min and that of the wild type was 175 min at 95°C. However, the thermostability of the mutant E41A, which has a $T_{1/2}$ value of 25 min at 95°C, was significantly decreased compared to the wild type of *Ap*SOD. To explain the enhanced thermostability of K12A and thermolabile E41A on the structural basis, the crystal structures of the two SOD mutants have been determined. The results have clearly shown the general significance of hydrogen bonds and ion-pair network in the thermostability of proteins.

Key Words: **thermostability; superoxide dismutase; *Aquifex pyrophilus;* hydrogen bonds; ion pair network.**

The structure and stability of a hyperthermophilic protein have attracted increasing attention in recent years. Hence, various groups identified the factors that determine protein stability by structural comparisons between mesophilic enzymes and hyperthermophilic proteins (1, 2). The basis of their stability includes hydrogen bonding networks, hydrophobic interactions, optimized core packing, salt bridges and the reduction of the entropy of unfolding (3). Even though a detailed understanding of protein-stabilization mechanism has not yet to be achieved, it is clear that thermostable proteins used these known interactions optimally rather than containing unique structural characteristics.

Perutz and Raidt (4) originally suggested salt bridges as a means of promoting the thermal stability, through the analysis of primary sequences of proteins from mesophiles. The recent results of high-resolution structures of some hyperthermophilic proteins have demonstrated that the number of surface ion-pairs is even greater than those of their mesophilic counterparts (5–7).

Our crystal structural studies of *Ap*SOD pointed out two significant factors for SOD hyperthermostability (8). First, a large number of ion-pair formation within the subunit of *Ap*SOD may be the most important as well as between subunits. Second, the increased numbers of hydrophobic and polar interactions at the enlarged buried subunit interface in tetramer may be a major factor for the stability of the quaternary structure of *Ap*SOD.

Although ion-pairs of *Ap*SOD are widely distributed over the subunit, most of the ion-pairs of *Ap*SOD are not connected by networks. Only two net works are found in the subunit, which one involving five residues and the other involving three residues. To identify the amino acid residues essential for the thermostability of the SOD from *Aquifex pyrophilus,* we designed two mutants of *Ap*SOD, K12A and E41A, in which Lys12 and Glu41 in *Ap*SOD ion-pair network were replaced by Ala. Replacement of Lys12 located in the L1 loop with Ala resulted in an increased thermostability. The substitution of the Glu41 located in α1 helix with Ala significantly decreased thermostability of SOD compared to the wild type.

Analysis of the X-ray crystal structure clearly showed the effect of a single alanine substitution on the thermostability of hyperthermophilic superoxide dismutase from *Aquifex pyrophilus.*

[1] To whom correspondence and reprint requests should be addressed at 39-1 Hawallkok-dong Sungbuk-ku, Seoul 130-650, Korea. Fax: +82 2 958 5939. E-mail: yshan2@kist.re.kr.

0006-291X/01 $35.00

MATERIALS AND METHODS

Cloning and Purification of SOD Mutants

Two mutants of *Ap*SOD, K12A and E41A, in which Lys12 and Glu41 in *Ap*SOD ion-pair network were replaced by Ala, were designed. Site directed mutagenesis was performed by inverted polymerase chain reaction. The clone, pD2, encoding the full length of *Ap*SOD was used as a template DNA (9). The reaction mixture contained 0.1 nM of each primer, 0.2 μM of dNTP mix, varying amounts of template DNA, 2.5 units of *Ex-Taq* polymerase (TAKARA, Japan) and the buffer supplied with the DNA polymerase in a total volume of 100 μl. The 25 cycles of amplification was performed as follows, 94°C for 30 s, 58°C for 30 s, and 72°C for 30 s. The PCR product was recovered from a low melting agarose gel electrophoresis and was digested with *Nde*I (or *Nco*I) and *Bam*HI. The products were ligated with pET3a/3d predigested with the same restriction enzymes. After confirming nucleotide sequence of the mutants, small-scale expression tests were performed and high level protein-expressing clones detected on an SDS polyacrylamide gel were chosen for large-scale protein purification. Cultivation of *E. coli* BL21(DE3) containing plasmids and purification of the mutant proteins were performed as described for wild type of *Ap*SOD (9).

Crystallization, Data Collection, and Processing

Crystals of two mutants were grown at room temperature by the hanging drop vapor diffusion method as previously described (8). The crystals belong to space group I222 with $a = 70.7$ Å, $b = 75.8$ Å, and $c = 86.9$ Å for K12A and $a = 70.6$ Å, $b = 75.5$ Å, and $c = 87.2$ Å for E41A, respectively. The data sets were collected from a MAR Research 300 image-plate detector mounted on a Rigaku RU-200 rotating-anode generator. The two mutant crystals diffract to 2.0 and 1.9 Å at room temperature, respectively. The data were processed using the programs DENZO and SCALEPACK (10). A summary of data collection, processing, and refinement is given in Table 1.

Structure Refinements and Analysis of Data

Refinement of K12A. The atomic coordinates of wild-type *Ap*SOD (1COJ) were used as the starting model for the refinement of K12A. The 10% reflections were used to calculate the R_{free} value to monitor the progress of the refinement (11). Without the mutated residue K12A, the *R*-factor dropped to 25% ($R_{free} = 31\%$) for 15,097 reflections in the resolution range 8–2.0 Å. Ala12 was then inserted and fitted into the difference electron density map, the model was subjected to simulated annealing by heating the system to 4000 K and slowly cooling to 300 K in steps of 25 K. The 100 cycles of positional refinement lowered the *R*-factor to 19% ($R_{free} = 23\%$). The iron ion was then included and water molecules were added from the difference electron density maps at various stages of the refinement. The current model contains 211 amino acid residues, an iron atoms and 114 water molecules in an asymmetric unit. The structure has an *R*-factor of 16.0% ($I > 2\sigma$) and R_{free} of 21.3% ($I > 2\sigma$) for data from 8 to 2.0 Å, with 0.008 Å RMS deviation from ideal bond lengths and 1.602 Å RMS deviation from the ideal bond angles (Table 1).

Refinement of E41A. The atomic coordinates of wild-type *Ap*SOD (PDB ID, 1SOD) were used as the starting model for the refinement of E41A. A randomly selected 10% of the reflections were used to calculate the R_{free} value to monitor the progress of the refinement (11). The refinement protocols as above gave a final *R*-factor of 16.3% ($R_{free} = 19.1\%$) for data from 8 to 1.9 Å ($I > 2\sigma$), including 115 water molecules with 211 amino acids and one iron atom. The bond RMS deviation is 0.007 Å and angle RMS deviation is 1.602 Å (Table 1).

Analysis of data. In all cases, the program X-plor 3.1 was used for the refinement and the program CHAIN was used for molecular modeling (11, 12). Hydrogen bonds and ion-pairs are analyzed using X-plor and confirmed visually on a Silicon graphics system using the program CHAIN. Hydrogen bond and ion-pair interactions were identified using distances less than or equal to 3.5 and 4.0 Å, respectively (13).

TABLE 1

Summary of Crystallographic Analysis

Data	K12A	E41A
Spacegroup	I222	I222
Cell parameters *a* (Å), *b* (Å), *c* (Å)	70.7, 75.8, 86.9	70.6, 75.5, 87.2
Maximum resolution (Å)	2.0	1.9
Observations ($>1\sigma$)	48,844	144,933
Unique reflections	15,598	18,703
R_{sym} (%)[a]	8.5	6.7
Completeness (%), refinement	96.6	99.9
Nonhydrogen atoms	1716 protein 1 Fe(III), 114 water	1716 protein 1 Fe(III), 115 water
R-factor[b] (R_{free})[c]	16.0% (21.3%)	16.3% (19.1%)
No. of reflections used in *R*-factor calculation ($I > 2\sigma$)	15,097	17,769
RMSD from ideal geometry		
Bond lengths (Å)	0.008	0.007
Bond angles (degree)	1.602	1.602
Dihedral angles (degree)	5.584	8.218
Improper angles (degree)	0.127	0.046

[a] $R_{sym} = \Sigma_h \Sigma_j |I_{h,i} - \langle I_h \rangle| / \Sigma_h \Sigma_i \Sigma I_{h,i}$, where $I_{h,i}$ is the intensity of the *i*th measurement of reflection *h* and ⟨Ih⟩ is the corresponding value of Ih for all *i* measurements.

[b] *R*-factor $= \Sigma \| F_{obs}| - |F_{calc} \| / \Sigma |F_{obs}|$, where F_{obs} and F_{calc} are the observed and calculated structure factors, respectively.

[c] R_{free} = *R*-factor calculated using 10% of the reflection data chosen randomly and omitted from the start of refinement.

Activity assay and thermostability measurements for the SOD mutants. SOD activity was measured by cytochrome *c* reduction (14). SOD activity unit is defined as the amount of enzyme which inhibits the rate of cytochrome *c* reduction by 50%. Protein concentration was measured by the method of Bradford (15). Thermal stability of SOD mutants were determined by the method as described before (9). Reaction mixtures containing 1 μg/μl of SOD in 20 mM potassium phosphate, pH 7.0, was incubated at 95°C. Aliquots were removed at intervals, chilled in an ice bath, and assayed the residual SOD activity.

RESULTS

Cloning and Purification of ApSOD Mutants

All SOD mutants were purified from the soluble fractions of the cell lysates and the purity was confirmed as a unique band in both native and SDS–polyacrylamide gel electrophoresis (Fig. 1). Properties of the mutants during the purification procedure were almost identical to that of the wild-type SOD. Each mutant has different mobility of dimer in SDS–polyacrylamide gel electrophoresis due to the one amino acid substitution (Fig. 1B). The different proportion of dimer to monomer between the K12A and E41A was shown in the SDS–

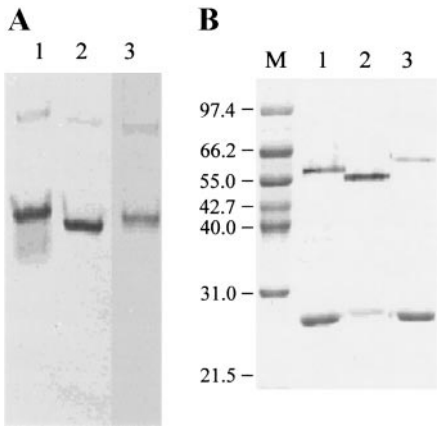

FIG. 1. Identification of SOD mutants on 10% nondenaturing (A) and 12.5% SDS–denaturing (B) polyacrylamide gel electrophoresis. The 10 μg of each proteins were applied on the two types of gel. In the case of SDS–PAGE, the samples were heated at 100°C for 10 min after mixing SDS loading buffer. M, molecular marker; 1, wild type of SOD; 2, mutant K12A SOD; 3, mutant E41A SOD.

polyacrylamide gel electrophoresis. The compactness of K12A could contribute to the different mobility compared to that of E41A and more proportion of dimer than monomer in the SDS–polyacrylamide gel electrophoresis. The yield of each mutant protein was 20~30 mg from 1 liter culture.

As shown in Table 2, the specific activity of the mutants were compared with that of wild type SOD when assayed at 25°C by the cytochrome *c* reduction method. The activity of SOD mutants—K12A and E41A—were greater than the wild type. It could not be interpreted as an effect of greater Fe incorporation, because the other mutant which also had more metal content than wild type did not have an increased activity (data not shown).

Thermostability of ApSOD Mutants

Heat inactivation assay was performed with constructed mutant of *Ap*SODs and wild type to compare the thermostability. The mutant E41A had lost 40% of its activity within 10 min at 95°C. As shown on Fig. 2 and Table 2, the mutant E41A showed distinctly decreased stability, supporting that ion-pair network has actually a critical role in stabilizing *Ap*SOD.

However, unexpectedly, thermostability of the mutant K12A, was increased compared with that of the wild type, the $T_{1/2}$ value of K12A was 210 min at 95°C, which is greater than that of the wild type, 175 min.

Structural Analyses of ApSOD Mutants

The structure of native *Ap*SOD has previously been refined to a high resolution of 1.9 Å (8). In a native protein, we have analyzed several structural factors that contribute to enzyme stability. The most striking features are the increased ion-pairs in the monomer and the increased buried surface area in the tetramer. This structure has been used as a standard for the comparison of the mutant *Ap*SOD structures in this work. When the structures of the mutants were superimposed with the native *Ap*SOD structure using the program LSQ from the CCP4 program suite (16), no significant deviations were observed among the main-chain atoms (RMS deviation for main-chain atoms is 0.13 Å for both mutants). In addition, strong electron density was observed for the iron atoms like a native structure. However, local changes around the mutated residues were found as shown in Fig. 3 and Fig. 4.

In the native *Ap*SOD structure, only two networks are found in the subunit; one involving five residues and the other involving three residues (Fig. 5). The five ion-pair network, which is located between L1 and α1 in the N-terminal domain, involves residues D9, K12, E25, E29, and K33 (Fig. 5). The NZ(K12) in the native *Ap*SOD, formed salt bridges with OE2 (E29), OE1(E25), and OE2(E25), which are relayed ion-pairs. However, in the K12A structure, a water molecule is located in CE position of K12 of wild-type *Ap*SOD such that it forms hydrogen bonds with two residues (E29, E25) instead of ion-pair network (Fig. 3). The W33 in the K12A structure was moved about 0.4 Å to W109 compared to that of wild type, so the interaction of W33 between Q14 and W109 have been increased than those of the wild type (Fig. 3). The interaction between W33 and Q14 could stabilize the local structure even further, which may account the increased stability of a mutant K12A. Therefore, K12A structure has a more

TABLE 2

Properties of the Mutant SODs Compared with That of Wild-Type SOD

mSOD	Substituted residue	Metal[a] Fe	Metal[a] Zn	Specific activity (units/mg)	$T_{1/2}$ (95°C) (min)	Location
Wild type	—	0.33	0.047	1250	75	
K12A	K12A	0.42	0.1	1500	210	L1/ion-pair network A
E41A	E41A	0.38	0.07	1330	25	α1/ion-pair network B

[a] The unit is atom per subunit.

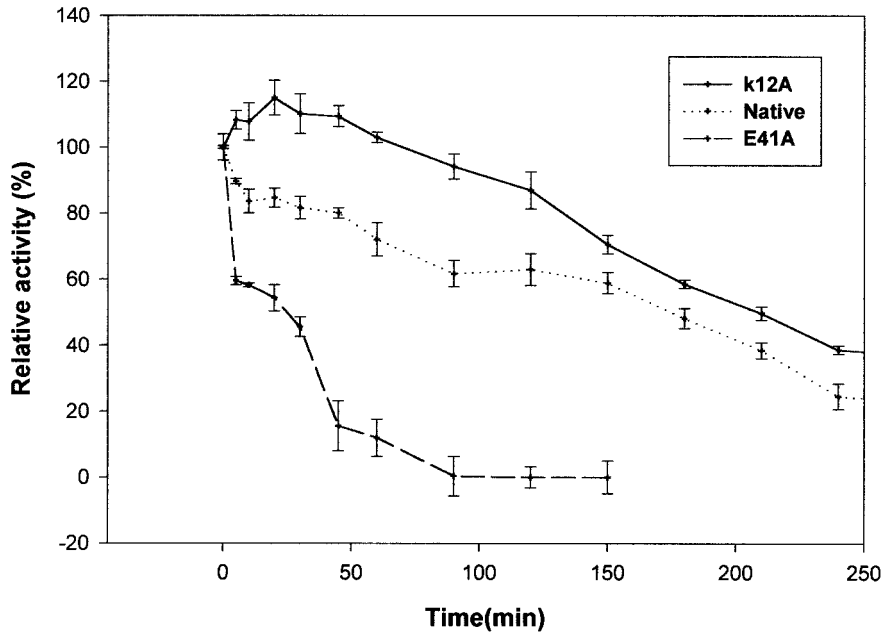

FIG. 2. Comparison of the thermostability among *Ap*SOD mutants. Solutions of wild-type and mutant *Ap*SOD (0.1 mg/ml) were heated at 95°C for various times in buffer containing 20 mM potassium phosphate. The remaining activity was assayed as described under Materials and Methods.

hydrophilic exterior and a more hydrophobic interior than wild-type *Ap*SOD in the tetrameric structure.

However, in the E41A structure, NZ(K45)-OE1(E41)-NZ(K38) ion-pair network of wild-type *Ap*SOD is disrupted (Fig. 4). Ion-pair is the important stabilizing forces in proteins (17). And also the energy gain in a network is larger than the sum of the pairwise interactions between the consistent charges (18). A water molecule is located in CE position of E41 of wild-type *Ap*SOD that it forms hydrogen bonds with two residues (K45 and K38) instead of ion-pair network (Fig. 4), but it is not as stable as the relayed ion-pairs in the native *Ap*SOD. The E41 is located on the position of ion-pair network in the intramolecular and intermolecular of the *Ap*SOD tetrameric structure. Therefore, the ion-pair network of this area is important in thermostability of the *Ap*SOD tetrameric structure.

There might be several other factors to contribute the thermostability of K12A and E41A besides the hydrogen bonds and ion-pair network. The intersubunit ion-pairs of the native *Ap*SOD and the mutants were compared, but any noticeable changes were not found. There was also negligible change of the solvent accessible surface area between the native *Ap*SOD and the mutants.

In summary, the structures of the mutants K12A and E41A show that the hydrogen bonds and ion-pair network play a key role in determining the thermostability of the *Ap*SOD. The results have clearly shown the general significance of hydrogen bonds and ion-pair network in the thermostability of proteins.

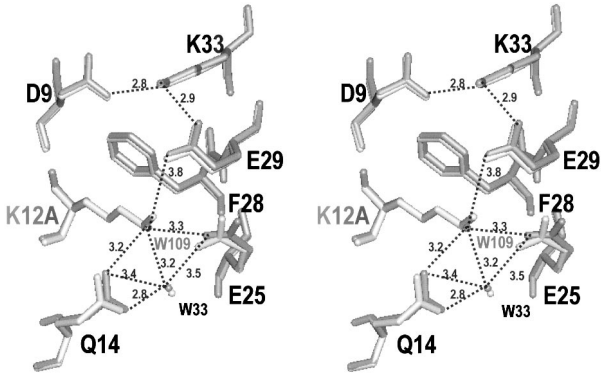

FIG. 3. Representation of residues involved in the ion-pair of mutant K12A. The native *Ap*SOD and the mutant K12A are shown.

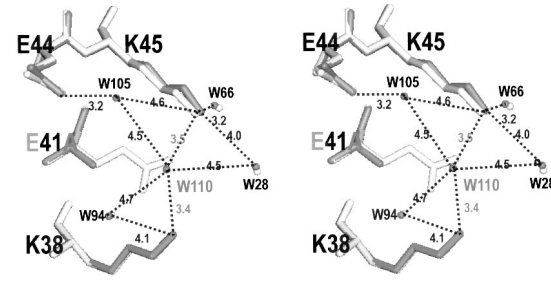

FIG. 4. Representation of residues involved in the ion-pair of mutant E41A. The native *Ap*SOD and the mutant E41A are shown.

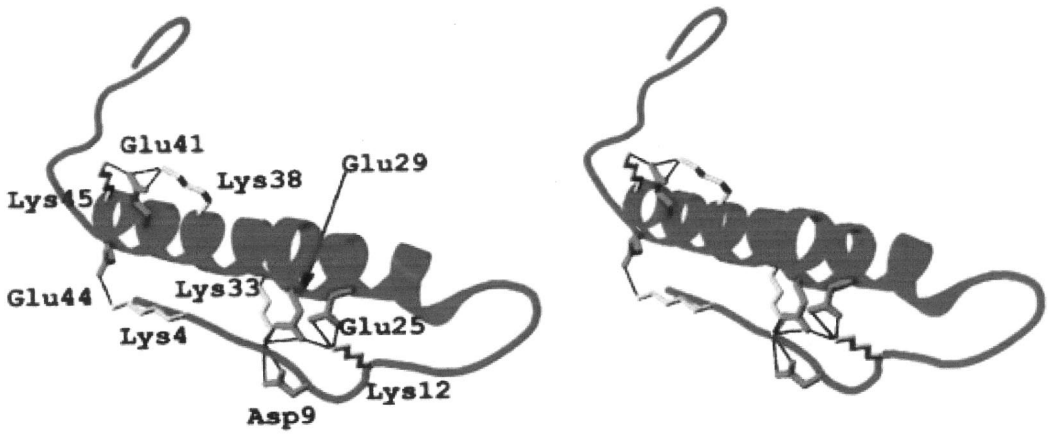

FIG. 5. Stereodiagram of the intra-subunit ion-pair networks in the N terminus of *Ap*SOD. Residues in loop L1 and the α 1 helix are involved in network formation.

DISCUSSION

The crystal structure of the enhanced thermostability of K12A and thermolabile E41A could give valuable factors responsible for the thermostability. In K12A structure, a water molecule is located in CE position of K12 of wild-type *Ap*SOD such that it forms hydrogen bonds with two residues—E29(OE2) and E25(OE2)—instead of salt bridges of K12 with E29 (OE2) and E25(OE1, OE2). A new bond between a water molecule and Q14(NE2) was formed in K12A structure. Even though salt bridges appear to make little contribution to protein stability at room temperature, they have been proposed to play a crucial role in promoting hyperthermostability in proteins (19). The apparently destabilizing effects of salt bridges at room temperature can be reconciled with their increased abundance in hyperthermophilic proteins. Many hyperthermophilic proteins have been shown to contain an increased number of salt bridges, involving in networks at interdomain interfaces and inter-subunit interfaces in the oligomeric proteins (1, 2, 7, 8). However, in K12A structure, two hydrogen bonds and a new interaction between a water molecule and Q14(NE2) contribute for the increased stability compared to the three relayed ion-pairs in the native *Ap*SOD. The effect of hydrogen bonds on RNase T1 stability was studied and found that individual hydrogen bond contributed an average of 1.3 kcal/mol to the stabilization (20). Tanner *et al.* showed that a strong correlation between GAPDH thermostability and the number of charged neutral hydrogen bond (21). One of the reasons why this type of hydrogen bond is thermodynamically stabilizing is that the desolvation penalty associated with burying such hydrogen bonds is less than the desolvation penalty for burying an ion pair that involves two charged residues. Among the hyperthermophilic proteins whose structures have been solved, hydrogen bonds in many proteins contribute to the thermostability (22).

In the E41A structure, NZ(K45)-OE1(E41)-NZ(K38) ion-pair network of wild-type *Ap*SOD is disrupted and a water molecule which is located in CE position of E41 of wild-type *Ap*SOD forms hydrogen bonds with two residues (K45 and K38) instead of ion-pair network. Since this hydrogen bond is not as stable as the relayed ion-pairs in the native *Ap*SOD, E41A was thermolabile compared to the native *Ap*SOD.

The contribution of hydrogen bonds (23, 24) and salt links (25, 26) to the stability of proteins is controversial. The removal of a hydrogen bond generally lowers protein stability by 0.5 to 2.0 kcal/mol and estimates for ion pair stabilization range from 0.4 to 1.0 kcal/mol (27, 28). The ion pair networks identified in the *P. furiosus*, *P. kodakaraensis*, and *T. litoralis* GDH structures, which are 83 to 87% identical and all contain the same 18 ion pair network at their hexamer interface, were studied by site directed mutagenesis (1, 29, 30). These studies illustrate the high level of cooperation among the different members of ion pair network and support the role of the 18-residue ion pair network in GDH stabilization.

The arrangement of charged residues into networks at high temperatures may play a key role in the acquisition of thermostability of proteins. The reasons are as follows:

First, the dielectric constant decreases significantly with temperature. Second, each new member in a network of ion-pairs requires the desolvation of just one residue. Third, hydration free energies are reduced at elevated temperatures and because these reductions are considerably larger for charged residues than for hydrophobic isosteres, ion-pairs may become more stabilizing than hydrophobic interactions at elevated temperatures (19, 31).

The disruption of ion-pair network of E41A was a crucial factor for the thermostability of the mutant E41A. In the SOD mutants case, K12A and E41A,

which were participated in the hydrogen bond and ion pair, make a different contribution for the thermostability.

ACKNOWLEDGMENTS

We gratefully acknowledge the financial support from the Korea Institute of Science and Technology and a grant from the Ministry of Science and Technology, Korea.

REFERENCES

1. Yip, K. S., Stillman, T. J., Britton, K. L., Artymiuk, P. J., Baker, P. J., Sedelnikova, S. E., Engel, P. C., Pasquo, A., Chiaraluce, R., and Consalvi, V. (1995) The structure of *Pyrococcus furiosus* glutamate dehydrogenase reveals a key role for ion pair networks in maintaining enzyme stability at extreme temperatures. *Structure* **3,** 1147–1158.
2. Korndörfer, I., Steipe, B., Huber, R., Tomschy, A., and Jaenicke, R. (1995) The crystal structure of holo-glyceraldehyde-3-phosphate dehydrogenase from the hyperthermophilic bacterium *Thermotoga maritima* at 2.5 Å resolution. *J. Mol. Biol.* **246,** 511–521.
3. Vieille, C., and Zeikus, J. G. (1996) Thermoenzymes, identifying molecular determinants of protein structural and functional stability. *Trends Biotechnol.* **14,** 183–189.
4. Perutz, M. F., and Raidt, H. (1975) Stereochemical basis of heat stability in bacterial ferredoxin and in haemoglobin A2. *Nature* **255,** 256–259.
5. Day, M. W., Hsu, B. T., Joshuator, L., Park, J. B., Zhou, Z. H., Adams, M. W. W., and Rees, D. (1992) X-ray crystal structures of the oxidised and reduced forms of the rubredoxin from the marine hyperthermophilic archaebacterium *Pyrococcus furiosus*. *Protein Sci.* **1,** 1494–1507.
6. Chan, M. K., Mukland, S., Kletzin, A., Adams, M. W., and Rees, D. C. (1995) Structure of hyperthermophilc tungstopterin enzyme, aldehyde ferredoxin oxidoreductase. *Science* **267,** 1463–1469.
7. Hennig, M., Darimont, B., Sterner, R., Kirschner, K., and Jansonius, J. N. (1995) 2.0 Å structure of indole-3-glycerol phosphate synthase from the hyperthermophile *Solfolobus solfataricus*, possible determinants of protein stability. *Structure* **3,** 1295–1306.
8. Lim, J. H, Yu, Y. G., Han, Y. S, Cho, S., Ahn, B. Y., Kim, S. H., and Cho, Y. (1997) The crystal structure of an Fe-superoxide dismutase from the hyperthermophile *Aquifex pyrophilus* at 1.9 Å resolution, structural basis for thermostability. *J. Mol. Biol.* **270,** 259–274.
9. Lim, J. H., Yu, Y. G., Choi, I-G., Ryu, J-R., Ahn, B-Y., Kim, S-H., and Han, Y. S. (1997) Cloning and expression of superoxide dismutase from *Aquifex pyrophilus*, a hyperthermophilic bacterium. *FEBS Lett.* **406,** 142–146.
10. Otwinowski, Z., and Minor, W. (1997) Processing of X-ray diffraction data collected in oscillation method. *Methods Enzymol.* **276,** 307–326.
11. Brünger, A. T. (1992) X-PLOR Version 3.1 (A system for X-ray Crystallography and NMR), Yale Univ. Press, New Haven and London.
12. Sacks, J. S. (1988) CHAIN, a crystallographic modeling program. *J. Mol. Graph.* **6,** 224–225.
13. Barlow, D. J., and Thomton, J. M. (1983) Ion-pairs in proteins. *J. Mol. Biol.* **168,** 867–885.
14. McCord, J. M., and Fridovich, I. (1969) Superoxide dismutase, an enzymatic function for erythrocuprein (hemocuprein). *J. Biol. Chem.* **244,** 6049–6055.
15. Bradford, M. (1976) A rapid and sensitive method for the quantitation of microgram quantities of protein utilizing the principle of protein–dye binding. *Anal. Biochem.* **72,** 248–254.
16. The *CCP*4 suite: Programs for protein crystallography Number 4 Collaborative Computational Project (1994) *Acta Cryst.* **D50,** 760–763.
17. Nakamura, H. (1996) Roles of electrostatic interaction in proteins. *Q. Rev. Biophys.* **29,** 1–90.
18. Horovitz, A., Serrano, L., Avron, B., Bycroft, M., and Fersht, A. R. (1990) Strength and co-operativity of contributions of surface salt bridges to protein stability. *J. Mol. Biol.* **216,** 1031–1044.
19. Elcock, A. H. (1998) The stability of salt bridges at high temperatures: Implications for hyperthermophilic proteins. *J. Mol. Biol.* **284,** 489–502.
20. Shirley, B. A., Stanssens, P., Hahn, U., and Pace, C. N. (1992) Contribution of hydrogen bonding to the conformational stability of ribonuclease T1. *Biochemistry* **31,** 725–732.
21. Tanner, J. J., Hecht, R. M., and Krause, K. L. (1996) Determinants of enzyme thermostability observed in the molecular structure of *Thermus aquaticus* D-glyceraldehyde-3-phosphate dehydrogenase at 2.5 Å resolution. *Biochemistry* **35,** 2597–2609.
22. Vieille, C., and Zeikus, G. J. (2001) Hyperthermophilic enzymes: Sources, uses, and molecular mechanisms for thermostability. *Microbiol. Mol. Biol. Rev.* **65,** 1–43.
23. Sippl, M. J., Ortner, M., Jaritz, M., Lackner, P., and Flockner, H. (1996) Helmholtz free energies of atom pair interactions in proteins. *Folding Des.* **14,** 289–298.
24. Pace, N. C., Shirley, B. A., McNutt, M., and Gajiwala, K. (1996) Forces contributing to the conformational stability of proteins. *FASEB J.* **10,** 75–83.
25. Dill, K. (1990) Dominant forces in protein folding. *Biochemistry* **29,** 7133–7155.
26. Sharp, K. A., and Honig, B. (1990) Electrostatic interactions in macromolecules. *Annu. Rev. Biophys. Chem.* **19,** 301–332.
27. Yang, A. S., and Honig, B. (1993) On the pH dependence of protein stability. *J. Mol. Biol.* **231,** 459–474.
28. Pace, N. C., Laurents, D. V., and Erikson, R. E. (1992) Urea denaturation of barnase: pH dependence and characterization of the unfolded state. *Biochemistry* **29,** 2564–2572.
29. Rahman, R. N. Z. A., Fujuwara, S., Nakamura, H., Takagi, M., and Imanaka, T. (1998) Ion pairs involved in maintaining a thermostable structure of glutamate dehydrogenase from a hyperthermophilic archaeon. *Biochem. Biophys. Res. Commun.* **248,** 920–926.
30. Vetriani, C., Maeder, D. L., Tolliday, N., Yip, K. S., Stillman, T. J., Britton, K. L., Rice, D. W., Klump, H. H., and Robb, F. T. (1998) Protein thermostability above 100°C: A key role for ionic interactions. *Proc. Natl. Acad. Sci. USA* **95,** 12300–12305.
31. Elcock, A. H., and McCammon, J. A. (1997) Continuum solvation model for studying protein hydration thermodynamics at high temperatures. *J. Phys. Chem.* **101,** 9624–9634.